0026-895X/04/6502-370–380$20.00
MOLECULAR PHARMACOLOGY
Vol. 65, No. 2
2541/1125140
Mol Pharmacol 65:370–380, 2004
Printed in U.S.A.

Use-Dependent Inhibition of the *N*-Methyl-D-aspartate Currents by Felbamate: a Gating Modifier with Selective Binding to the Desensitized Channels

Chung-Chin Kuo, Bei-Jung Lin, Huai-Ren Chang, and Chi-Pan Hsieh

Department of Physiology, National Taiwan University College of Medicine, Taipei, Taiwan (C.-C.K., B.-J.L. H.-R.C., C.-P.H.); and Department of Neurology, National Taiwan University Hospital, Taipei, Taiwan (C.-C.K.)

Received March 24, 2003; accepted October, 31, 2003

This article is available online at http://molpharm.aspetjournals.org

ABSTRACT

Felbamate (FBM) is a potent nonsedative anticonvulsant whose clinical effect may be related to the inhibition of *N*-methyl-D-aspartate (NMDA) currents, but the exact molecular action remains unclear. Using whole-cell patch-clamp recording in rat hippocampal neurons, we found that submillimolar FBM effectively modifies the gating process of NMDA channels. During a single high-concentration (1 mM) NMDA pulse, FBM significantly inhibits the late sustained current but not the early peak current. However, if the 1 mM NMDA pulse is preceded by a low-concentration (10 μM) NMDA prepulse, then FBM significantly inhibits both the peak and the sustained currents in the 1 mM pulse. In sharp contrast, the NMDA currents elicited by micromolar NMDA are only negligibly inhibited or even enhanced by FBM. These findings indicate that the inhibitory effect of FBM on NMDA currents is stronger with both higher NMDA concentration and longer NMDA exposure, and is thus "use-dependent". FBM also slows recovery of the desensitized NMDA channel, and quantitative analyses of FBM effects on the activation kinetics and the desensitization curve of the NMDA currents further disclose dissociation constants of ~200, ~110, and ~55 μM for FBM binding to the resting, activated, and desensitized NMDA channels, respectively. We conclude that therapeutic concentrations (50–300 μM) of FBM could bind to and modify a significant proportion of the resting NMDA channel even when NMDA or other glutamatergic ligand is not present and then decrease the NMDA currents at subsequent NMDA pulses by stabilization of the desensitized channels. Because the inhibitory effect is apparent only when there is excessive NMDA exposure, FBM may effectively inhibit many seizure discharges but preserve most normal neuronal firings.

Felbamate (FBM; 2-phenyl-1,3-propanediol dicarbamate) is a potent new-generation anticonvulsant that is effective against many different types of epilepsy (Pellock and Brodie, 1997). In addition to clinical cases, the broad-spectrum antiepileptic effect is also well documented in experimental seizures. For example, FBM is effective against both supramaximal extension seizures induced by maximal electroshock and threshold seizures induced by pentylenetetrazol (Swinyard et al., 1986). Although serious complications such as aplastic anemia and hepatotoxicity have limited its use, FBM is an anticonvulsant which is too important to discard. With informed consent of the patients, FBM has remained as a useful anticonvulsant for Lennox-Gastaut syndrome in children and for a variety of complex partial seizures that are refractory to the other anticonvulsants in adults (Kaufman et al., 1997; Pellock, 1999).

The intriguing pharmacological profile of FBM implies a unique mechanism of action. Just as for the other nonsedative anticonvulsants, any proposed mechanism underlying FBM action preferably should explain why seizure discharges are effectively inhibited but normal neuronal firings are relatively preserved. FBM has been reported to have multiple pharmacological effects in native and cloned ion channels. As described previously, ~1 mM FBM inhibited cloned voltage-gated Na^+ channels from rat brain (Taglialatela et al., 1996). In addition, 1 to 3 mM FBM potentiated $GABA_A$ receptor current (Rho et al., 1994, 1997). On the other hand, very low concentrations of FBM inhibited up to ~40% of high-voltage–activated Ca^{2+} currents in rat cortical

This work was supported by grant NSC-90-2320-B-002-154 from the National Science Council, Taiwan. Huai-Ren Chang and Chi-Pan Hsieh are recipients of M.D. Ph.D./D.D.S. Ph.D. Predoctoral Fellowships DD9101N and DD9102C90, respectively, from the National Health Research Institute, Taiwan.

ABBREVIATIONS: FBM, felbamate; NMDA, *N*-methyl-D-aspartate; DCKA, dichlorokynurenic acid; C, closed (resting) state of the channel; O, open (activated) state of the channel; D, desensitized state of the channel; CF, OF, and DF, felbamate-bound closed, open, and desensitized states with dissociation constants $K_{f,c}$, $K_{f,o}$, and $K_{f,d}$ for each binding reaction, respectively; CN and CN_2, closed channels bound with one and two NMDA molecules, respectively.

neurons (IC_{50} = 504 nM) (Stefani et al., 1996). In this regard, it should be noted that the clinical effect of FBM usually requires a therapeutic dosage of 2400 to 3600 mg/day, which results in plasma or brain FBM concentrations of 50 to 300 μM (mean, ~150 μM) (Leppik et al., 1991; Theodore et al., 1991; The Felbamate Study Group in Lennox-Gastaut Syndrome, 1993; Adusumalli et al., 1994). In addition, reduction of seizure frequency is generally well correlated with FBM concentration in this range (The Felbamate Study Group in Lennox-Gastaut Syndrome, 1993). The FBM concentrations in the preceding experiments are far beyond or below the therapeutic range. Moreover, it is hard to envisage why FBM could differentiate between normal and seizure discharges with those experimental findings.

FBM may inhibit *N*-methyl-D-aspartate (NMDA) currents. In hippocampal slices, 50 to 100 μM FBM reduces NMDA receptor-mediated postsynaptic potentials (Pugliese et al., 1996). In cultured cortical neurons, 300 μM FBM shows significant neuroprotective effect by decreasing NMDA-induced neuronal injury (but not kainate-induced neuronal injury) (Kanthasamy et al., 1995). On the other hand, it has been shown that recombinant NR1-2B channels were more sensitive to FBM inhibition than were NR1-2A and NR1-2C channels. However, the IC_{50} values were all in the millimolar range (0.93–8.56 mM) (Kleckner et al., 1999). The exact cause of the big differences in effective FBM concentrations among different studies as well as the molecular mechanism underlying these effects of FBM is unclear.

FBM has been shown to slightly decrease single-channel NMDA currents or inhibit steady-state binding of [^{3}H]dizocilpine (an open NMDA channel blocker), suggesting a pore-blocking effect. However, it always takes millimolar (1–3 mM) FBM to do so (Rho et al., 1994; Subramaniam et al., 1995). On the other hand, McCabe et al. (1993) showed that FBM decreased [^{3}H]5,7-dichlorokynurenic acid (DCKA, a high-affinity glycine site antagonist) binding to the NMDA channels (IC_{50} = 374 μM) (Subramaniam et al., 1995). However, increase of glycine concentration failed to reverse FBM block. Instead, FBM increases [^{3}H]glycine binding to NMDA channels (EC_{50} = 485 μM in the rat and 142 μM in the human brain) (McCabe et al., 1998). These complicated or even seemingly contradictory data may be viewed as ambiguous evidences suggesting delicate interactions between therapeutic concentrations of FBM and the glycine site, a site notably involved in the gating conformational changes of the NMDA channel protein. To investigate the mechanism underlying the therapeutic effect of FBM, we studied the possible role of FBM as an NMDA channel-gating modifier in more detail. We found that FBM selectively binds to the activated, and especially to the desensitized NMDA channels. The selective binding may significantly contribute to the use-dependent block of the NMDA currents and consequently to the nonsedative anticonvulsant effect of FBM.

Materials and Methods

Cell Preparation. Coronal slices of the whole brain were prepared from 7- to 14-day-old Wistar rats. Hippocampal CA1 region was dissected from the slices and cut into small chunks. After treatment for 5 to 10 min at 37°C in dissociation medium (82 mM Na_2SO_4, 30 mM K_2SO_4, 3 mM $MgCl_2$, 5 mM HEPES, and 0.001% phenol red indicator, pH = 7.4) containing 0.5 mg/ml trypsin (type XI; Sigma, St. Louis, MO) or 3 mg/ml protease XXIII (Sigma), tissue chunks were moved to dissociation medium containing no trypsin but 1 mg/ml bovine serum albumin (Sigma) and 1 mg/ml trypsin inhibitor (type II-S, Sigma). Each time when cells were needed, two to three chunks were selected and triturated to release single neurons.

Whole-Cell Recording. The dissociated neurons were put in a recording chamber containing Tyrode's solution (150 mM NaCl, 4 mM KCl, 2 mM $MgCl_2$, 2 mM $CaCl_2$, and 10 mM HEPES, pH = 7.4). Whole-cell voltage-clamp recordings were obtained using pipettes pulled from borosilicate micropipettes (outer diameter, 1.55–1.60 mm) (Hilgenberg, Malsfeld, Germany), and fire-polished. The pipette resistance was 1 to 2 MΩ when filled with the internal solution containing 75 mM CsCl, 75 mM CsF, 10 mM HEPES, and 5 mM EGTA, with pH adjusted to 7.4 by CsOH. A seal was formed, and the whole-cell configuration was obtained in Tyrode's solution. The cell was then lifted from the bottom of the chamber and moved in front of a set of square glass three-barrel tubes (0.6 mm internal diameter) (Warner Instrument, Hamden, CT) or θ glass tubes (2.0 mm outer diameter pulled to an opening of ~300 μm in width) (Warner Instrument) emitting either control or FBM-containing external recording solutions whose basic components are Mg^{2+}-free Tyrode's solution and 0.5 μM tetrodotoxin. The glass-tube holder was connected to a stepper motor (SF-77B perfusion system, Warner Instrument) to achieve fast switch between different tubes and therefore rapid solution change. The rate of solution change was assessed by the rate of change in current size between two different external solutions containing different cations, namely Tyrode's solution and a solution containing 150 mM *N*-methyl-D-glucamine instead of 150 mM Na^+. The 50% current change time is shorter with the θ glass (~6 ms) than with the square glass (~40 ms) (Fig. 1). θ Glass tubes were therefore used in the experiments investigating the FBM effect on channel activation in Fig. 4, where a better resolution in the time domain is required. In the other experiments, square glass tubes were used because a greater number of different kinds of external solutions can be loaded at the same time. FBM (Tocris Cookson Inc., Bristol, UK) was dissolved in dimethyl sulfoxide to make a 100 mM stock solution. NMDA and glycine (Sigma) were dissolved in water to make 100 mM and 10 mM stock solutions, respectively. The stock solutions were then diluted into Mg^{2+}-free Tyrode's solution to attain the final concentrations desired (10 μM to 1 mM FBM, 0.1 μM to 1 mM NMDA, 0.3–30 μM glycine). The highest FBM concentration used in this study was 1 mM, which is close to its maximal solubility in water (~2–3 mM). However, the data in 1 mM FBM are only presented with bar graphs to show the tendency of current change over a wide concentration range of FBM (Figs. 2, B and C, and 5, B and C), and no further quantitative analysis is attempted on these bar graphs. For all detailed quantitative analyses, 300 μM is the highest FBM concentration included because millimolar FBM may start to have a pore-blocking effect (Rho et al., 1994; Subramaniam et al., 1995) and affect the accuracy of analysis. The final concentration of dimethyl sulfoxide (1% or less) was not found to have detectable effect on NMDA currents. The cells were voltage-clamped at −70 mV unless otherwise specified. NMDA currents were recorded at room temperature (~25°C) with an Axoclamp 200A amplifier, filtered at 1 kHz with a four-pole Bessel filter, digitized at 200- to 500-μs intervals, and stored using a Digidata-1200 analog/digital interface along with the pCLAMP software (all from Axon Instruments, Union City, CA).

Results

FBM Chiefly Inhibits the Sustained but not the Peak Currents Elicited by a Single Pulse of NMDA. Figure 2A shows that the NMDA currents (elicited with 1 mM NMDA and 0.3 μM glycine) in hippocampal neurons are significantly inhibited by 100 μM FBM, and the inhibition is even more pronounced with 1 mM FBM, demonstrating dose-dependence of FBM action. Most interestingly, closer examination

of the current sweeps reveals that the inhibitory effect is apparent chiefly on the late-sustained part of the NMDA current, but it is much less evident on the early-peak part of the current. In addition, the rising phase of NMDA currents seems to be accelerated rather than slowed in the presence of FBM (Fig. 4). On the other hand, the macroscopic deactivation kinetics after the NMDA pulse seems to have no significant change in the presence of FBM. The stronger inhibitory effect of FBM on the late-sustained currents than on the early-peak currents are confirmed by the cumulative results in Fig. 2B, clearly demonstrating that the inhibitory effect of

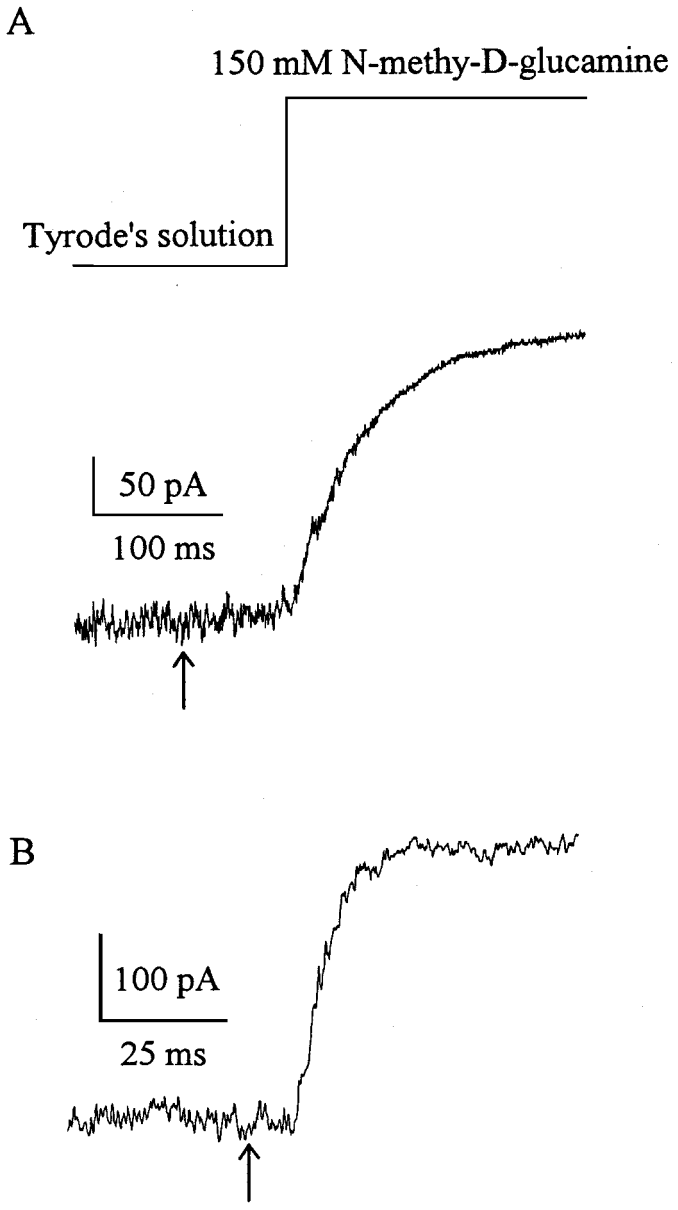

Fig. 1. Examination of the speed of solution change with the perfusion system. The cell was held at −40 mV and was exposed to 1 mM NMDA for 4 s every 35 s. At the middle of each NMDA pulse, the external solution was changed from Tyrode's solution to a solution containing 150 mM *N*-methyl-D-glucamine instead of 150 mM Na^+. The time course of changes in the current amplitude is taken as an indicator of the speed of external solution change with the perfusion system. A, solution change with the square glass. The arrow indicates the time point at which the electronic command of solution change is given. There is a latent period (~80 ms) between the electronic command and the point at which the current starts to change in this cell. Once the current starts to change, it takes ~40 ms to reach 50% of total change. B, solution change with the θ glass tube. The arrow has the same meaning as in part A, and here the latent period is only ~9 ms. Once the current starts to change, it takes ~6 ms to reach 50% of total change.

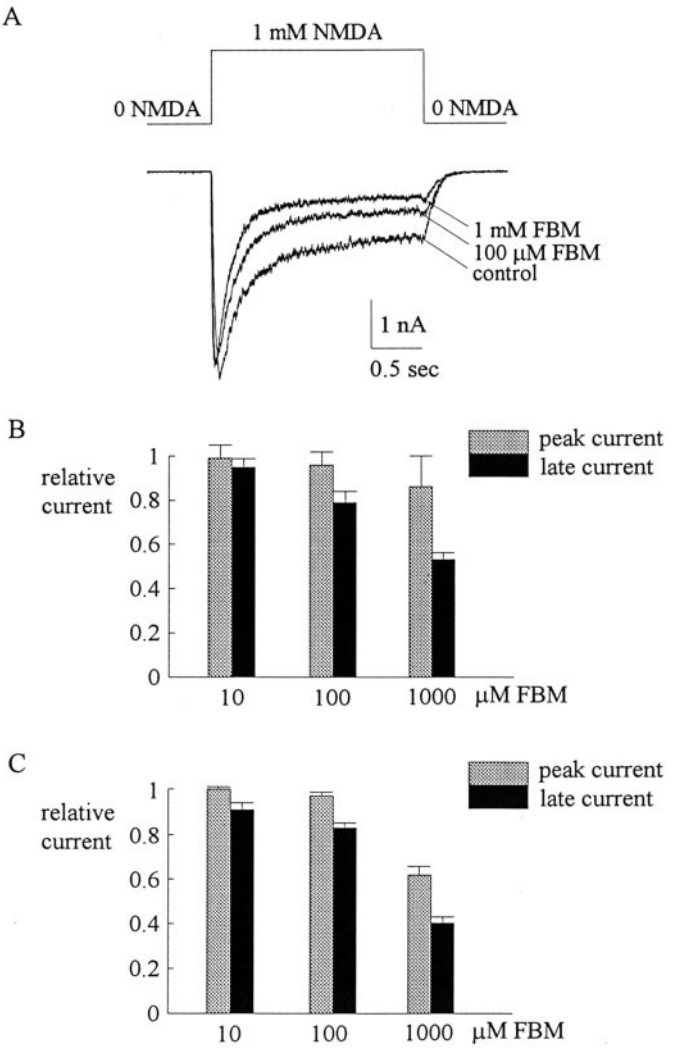

Fig. 2. FBM inhibition of NMDA current elicited by single NMDA pulse. A, every 35 s, the cell was moved from the NMDA- and glycine-free external solution to the external solution containing 1 mM NMDA and 0.3 μM glycine for 2 s, and then it was moved back to the NMDA-free external solution. The same concentrations of FBM were added to both external solutions if it was present in the system. Note the dose-dependent inhibition of the late-sustained NMDA currents by FBM. In contrast, FBM has little inhibitory effect on the early-peak currents. Also, note that both the initial rising phase and the decay phase of the NMDA currents seem to be accelerated in the presence of FBM. B, cumulative results are obtained from three cells with the experimental protocol described in A. The relative current is defined by the ratio between the amplitude of the currents elicited by the 1 mM NMDA pulse in FBM-containing and FBM-free external solutions in the same cell. For the peak currents, the relative currents are 0.99 ± 0.06, 0.96 ± 0.06, and 0.86 ± 0.14 in the presence of 10, 100, and 1000 μM FBM, respectively. For the late currents, the relative currents are 0.95 ± 0.04, 0.79 ± 0.05, and 0.48 ± 0.02 in the presence of 10, 100, and 1000 μM FBM, respectively. C, the same experiment as that described in A was repeated in seven cells, but the glycine concentration during the 2-s 1 mM NMDA pulse was increased to 30 μM. The relative current has the same definition as in B. For the peak currents, the relative currents are 1 ± 0.01, 0.97 ± 0.01, and 0.62 ± 0.04 in the presence of 10, 100, and 1000 μM FBM, respectively. For the late currents, the relative currents are 0.91 ± 0.03, 0.83 ± 0.02, and 0.41 ± 0.02 in the presence of 10, 100, and 1000 μM FBM, respectively.

FBM is closely dependent on the FBM concentration and the NMDA exposure time. Because there may be delicate interactions between FBM and glycine (see Introduction), we repeated the same experiments in the presence of saturating concentrations of glycine (30 μM glycine) (Fig. 2C). Despite slight quantitative differences, the findings in Fig. 2, B and C, are roughly similar, with both showing much more pronounced FBM inhibition of the late-sustained currents than of the early-peak currents. The NMDA exposure time-dependent inhibitory effect of FBM thus is a valid observation for a wide concentration range (from subsaturating to saturating concentrations) of glycine. We chose to use subsaturating concentration of glycine (0.3 μM) in most of the following experiments so that we might have the greatest chance to observe all gating modification effects of FBM on the NMDA channel, whether FBM synergistically or antagonistically interacts with glycine.

Submillimolar FBM Is Not an Effective Open NMDA Channel Blocker. It is intriguing why FBM shows different inhibitory effects on the early and late NMDA currents. If FBM blocks ion permeation through the pore, then the differential inhibitory effect would suggest that it is an open channel blocker. In other words, the FBM-binding site should be formed after the NMDA channel is open. Because FBM binding to this site needs time, the early-peak current would be less affected than the late current. If this is true, then the decay of NMDA currents in the presence of FBM should be ascribable to both channel desensitization and FBM binding, and there should be a positive correlation between FBM concentration and the macroscopic decay rate (e.g., linear correlation assuming simple bimolecular reaction between the drug and the channel). Figure 3 examines the relationship between FBM concentration and the macroscopic decay rate of NMDA currents. It is evident that the decay rate increases as FBM concentration increases from 0 to 300 μM but then remains roughly the same in 300 to 1000 μM FBM. The saturation of the decay rates with increasing FBM concentration, along with the accelerated rising phase of the NMDA currents in FBM (Figs. 2A and 4), would strongly argue against submillimolar FBM inhibiting NMDA currents as an open channel blocker. The accelerated decay of the macroscopic currents thus is more likely to be ascribable to the modified gating kinetics. In other words, the FBM-bound channel seems to desensitize more rapidly. From the simplified scheme in Fig. 3B, top, the data in Fig. 3A would then indicate that the reactions O to D and OF to DF roughly proceed with macroscopic speeds of 3.2 and 5.4 s^{-1}, respectively. In this regard, the macroscopic decay rates in different concentrations of FBM should be a weighted average of the decay rates of the FBM-bound and the FBM-free channels. We therefore tried to describe the data points in Fig. 3A with a rectangular hyperbola, which gives an apparent dissociation constant of 174 μM. This value could be viewed as a rough estimate of the binding affinity between FBM and the resting NMDA channels, with somewhat "contamination" by the affinity between FBM and the open NMDA channels. This is because the distribution of NMDA channels in the FBM-bound and the FBM-free forms in this experiment would be largely determined by the relative steady-state distribution of the NMDA channel in state C and in state CF when the cell is preincubated with FBM before the NMDA pulse. However, after the beginning of the NMDA pulse,

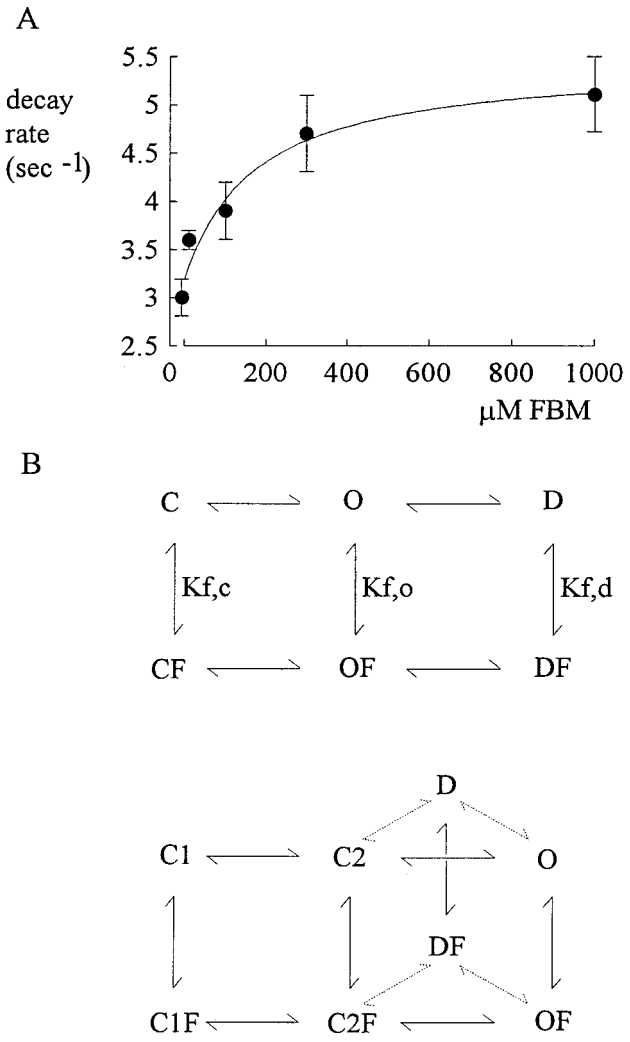

Fig. 3. Acceleration of the decay phase of NMDA currents by FBM. A, the experimental protocol is similar to that described in Fig. 2A. The decay phase of the macroscopic NMDA currents is fitted with a monoexponential decay function, and the inverse of the time constant from the fit is defined as the decay rate. The cumulative results of the decay rates are plotted against FBM concentration (n = 3–7). The line is the best rectangular hyperbola fit to the mean values of the decay rates and is of the following form: decay rate (s^{-1}) = ((2.2 s^{-1} × ([FBM]/174))/(1 + ([FBM]/174))) + 3.2 s^{-1}, where [FBM] denotes the FBM concentration in micromolar. B, two simplified gating schemes of the NMDA channel. Top, C, O, and D represent closed (resting), open (activated), and desensitized states of the channel, respectively. The signs of NMDA binding are omitted here for simplicity (see Fig. 6A for a more complete scheme in this regard). CF, OF, and DF are FBM-bound C, O, and D states, with dissociation constants $K_{f,c}$, $K_{f,o}$, and $K_{f,d}$ for each binding reaction, respectively. Bottom, C1 and C2 are the fully deactivated and the partially activated (but still closed) states, respectively. O and D have the same meaning as those at top, and the signs of NMDA binding are also omitted here. C1F, C2F, OF, and DF are FBM-bound C1, C2, O, and D states, respectively. The broken lines connecting states O and D, states OF and DF, states C2 and D, and states C2F and DF signal the unsettled debate that channel desensitization either tends to happen from the open state (Lin and Stevens, 1994) or exclusively happens from a partially activated but still closed state (Colquhoun and Hawkes, 1995). However, in either proposal, there is a similar basic rationale that NMDA channel activation and desensitization are both gating processes favored by NMDA binding and thus must be "coupled" to some extent. Although the scheme at bottom is more commonly used, it is also more complicated. We choose to focus on the basic linear C-O-D model (top) for future analyses so that the essence of possible coupling between channel activation and desensitization may be illustrated and the experimental data can be quantitatively treated with the greatest simplicity. Because most of the analyses in this study are from steady-state considerations, the major conclusions should remain similar if one chooses to use some other more complicated schemes like the one at the bottom.

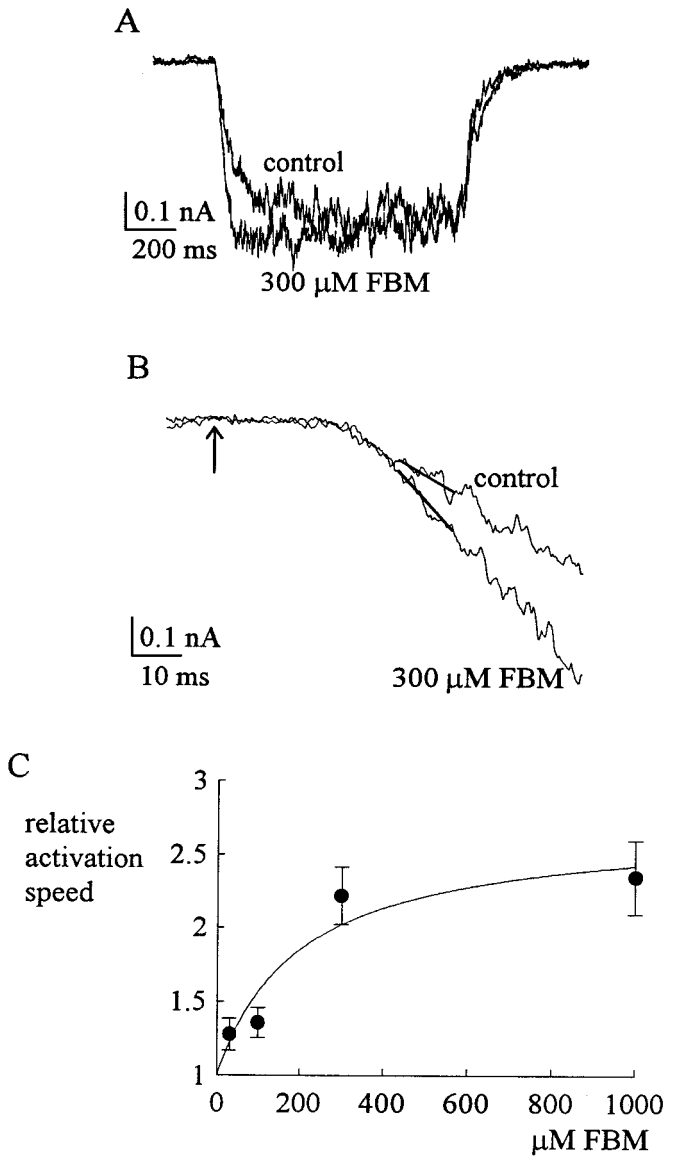

Fig. 4. Acceleration of the activation kinetics by FBM. A, every 60 s, the cell was moved from the NMDA- and glycine-free external solution to the external solution containing 10 μM NMDA and 0.3 μM glycine for 1 s, and then it was moved back to the NMDA-free external solution. FBM is either absent in both external solutions (the control sweep), or different concentrations of FBM are added only to the NMDA-free but not the NMDA-containing external solutions (e.g., the 300 μM FBM sweep). The very early NMDA current is evidently enhanced rather than inhibited by 300 μM FBM because of the accelerated rising phase. B, the rising phase of the currents is enlarged to illustrate the accelerated channel activation in more detail. The arrow indicates the time point at which the command of solution change is given electronically. The current between 35 and 45 ms from the arrow is fitted with a linear regression function to obtain the slope of current increase (in the unit of pA/ms). This time window is a deliberately chosen "compromise", because it should be as late as possible to avoid the period of incomplete solution change and also probable initial delay in channel activation (according to Fig. 1, solution change should be complete within 30 ms of the electronic command with θ glass tube) but as early as possible to avoid contamination of channel desensitization. C, in each individual cell, the slope of current increase in different concentrations of FBM is normalized to the slope in the control (FBM-free) solution to give the relative activation speed. The cumulative results of the relative activation speed from six to eight cells are plotted against FBM concentration. The line is the best rectangular hyperbola fit to the mean values and is of the following form: relative activation speed = 1 + (1.7([FBM]/200)/(1 + ([FBM]/200))), where [FBM] denotes FBM concentration in micromolar.

some NMDA channels may have been activated before the decay phase of the macroscopic current. FBM interaction with the open channel could then occur and somewhat alters the original steady-state distribution between states C and CF.

Felbamate Binds to the Resting NMDA Channel with a Dissociation Constant of ~200 μM. We have noted that the activation kinetics are accelerated in the presence of 100 to 1000 μM FBM (Fig. 2A). To characterize this intriguing phenomenon in more detail and to have a more accurate ("noncontaminated") measurement of the affinity between FBM and the resting NMDA channel, we first exposed the neuron to different concentrations of FBM in the absence of NMDA. The external solution was then quickly changed to the other one containing NMDA but not FBM, and the initial activation kinetics of the elicited NMDA current were measured. If the accelerated activation is another modified gating kinetic feature of the FBM-bound channel, the extent of acceleration of activation would be closely correlated with the extent of FBM binding to the resting NMDA channel during the pre-exposure to FBM (i.e., the relative distribution of channels between states C and CF in Fig. 3B). Because the measured parameter is the activation rather than the desensitization kinetics, and also because FBM was no longer present when NMDA was given to activate the channel, the measurement should be a more "pure" estimate of the affinity between FBM and the resting NMDA channels ($K_{f,c}$ in Fig. 3B). Figure 4, A and B, demonstrates acceleration of the initial activation phase of the currents in 300 μM FBM. Figure 4C shows that the accelerating effect is FBM dose-dependent and could be reasonably described by a one-to-one binding (simple bimolecular reaction) curve, giving a rough estimate of the dissociation constant of ~200 μM between FBM and the resting NMDA channel, and a ~1.7-fold faster activation speed for the FBM-bound (versus the FBM-free) resting NMDA channels. It is interesting that this number (~200 μM) is close to but slightly larger than the ~174 μM in Fig. 3A. This is conceivable because the measurement in Fig. 4 is less contaminated by FBM binding to the activated NMDA channel. The two different approaches thus give consistent results on the binding affinity of FBM to the resting channels and may also imply a slightly higher affinity between FBM and the open NMDA channels.

FBM Significantly Inhibits Peak Currents if the Neuron Is Prepulsed with NMDA. If submillimolar FBM is not an open channel blocker but is an effective gating modifier, then the much more pronounced inhibition of the late-sustained than the early-peak NMDA currents may suggest that FBM has a higher affinity to and thus stabilizes a nonconducting gating state that is favored by prolonged exposure to NMDA, namely the desensitized state. We examine such a possibility in Fig. 5. In the continuous presence of different concentrations of FBM, the neuron was first exposed to low concentrations (e.g., 10 μM) of NMDA for 5 s, driving part of the NMDA channels into the desensitized state. The NMDA concentration was then quickly switched to 1 mM to elicit current from channels that remained available (i.e., not desensitized) at the end of the 5-s prepulse of 10 μM NMDA. It is evident that in the same 1 mM NMDA pulse, 100 μM to 1 mM FBM has a much stronger inhibitory effect on the early-peak currents if there is a prepulse, whereas the effect of FBM on the late currents remains similar whether

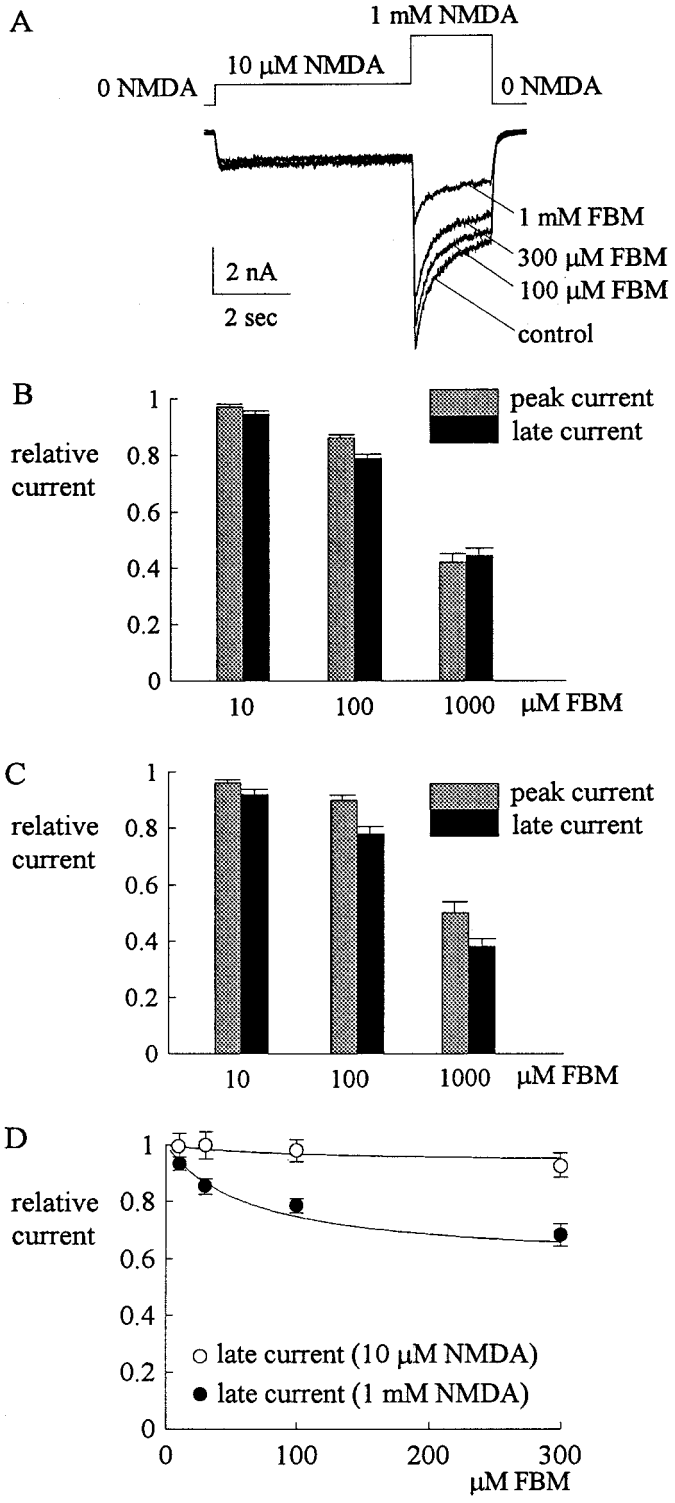

Fig. 5. FBM inhibition of NMDA currents elicited by two consecutive NMDA pulses. A, every 35 s, the cell was moved from the NMDA- and glycine-free external solution to the external solution containing 10 μM NMDA and 0.3 μM glycine for 5 s (the "10 μM NMDA prepulse"), then moved to another external solution containing 1 mM NMDA and 0.3 μM glycine for 2 s (the "1 mM NMDA pulse"), and then moved back to the NMDA-free external solution. The same concentration of FBM is added to both the NMDA-free and the NMDA-containing external solutions if it is present in the system. Note the significant inhibition of both the peak and the sustained currents by 100 μM to 1 mM FBM during the 1 mM NMDA pulse. In contrast, the same amount of FBM produces much less inhibition of the currents in the 10 μM NMDA prepulse. B, cumulative results are obtained from eight cells with the experimental protocol described in part A. The relative current is defined by the ratio between the amplitude of the currents elicited by the 1 mM NMDA pulse in the FBM-containing and the FBM-free external solutions in the same cell. For the early-peak currents, the relative currents are 0.97 ± 0.01, 0.88 ± 0.01, and 0.42 ± 0.03 in the presence of 10, 100, and 1000 μM FBM, respectively. For the late-sustained currents, the relative currents are 0.94 ± 0.01, 0.79 ± 0.01, and 0.45 ± 0.02 in the presence of 10, 100, and 1000 μM FBM, respectively. C, the same experiment as that described in part B was repeated in eight cells, but the glycine concentration in both 10 μM NMDA prepulse and 1 mM NMDA pulse was increased to 30 μM. The relative current has the same definition as that described in part B. For the peak currents, the relative currents are 0.96 ± 0.01, 0.90 ± 0.02, and 0.50 ± 0.04 in the presence of 10, 100, and 1000 μM FBM, respectively. For the late currents, the relative currents are 0.92 ± 0.02, 0.78 ± 0.03, and 0.38 ± 0.03 in the presence of 10, 100, and 1000 μM FBM, respectively. D, FBM produces much less inhibition of the NMDA currents in a 10 μM than in a 1 mM NMDA pulse. The relative late-sustained currents during the exposure to 10 μM NMDA are obtained from the same cells by the same method as that described in part B. The relative late-sustained currents in 1 mM NMDA are also plotted here for comparison. The lines are theoretical predictions of the data with eq. 3 and K_n and p values of 34 μM and 2.6, respectively (see text and Fig. 6 for detail).

the 10 μM NMDA prepulse is present or not (Figs. 2B and 5B). The stronger effect of FBM on the peak currents with pre-exposure to NMDA is consistent with the proposal that FBM stabilizes (increases) the desensitized channels and thus decreases the available channels at the end of the prepulse. The similar inhibitory effects on the late-sustained currents with or without the 5-s NMDA prepulse would further suggest that the inhibitory effect we documented in Fig. 2 is close to a steady-state condition. Most interestingly, there is a nearly negligible inhibitory effect of FBM on the late current directly elicited by 10 μM NMDA (Fig. 5A, during the prepulse). This is in sharp contrast to the significant inhibitory effect of FBM on NMDA currents directly elicited by 1 mM (Fig. 2A). Along with the very different inhibitory effects of FBM at the end of the 10 μM NMDA prepulse and at the beginning of the subsequent 1 mM NMDA pulse, these observations would strongly argue that the inhibitory effect of FBM is NMDA concentration-dependent and thus is more likely to be ascribable to gating modification of the channel rather than simple pore block. We once more repeated the same experiments in the presence of saturating concentrations of glycine (30 μM glycine) (Fig. 5C). Despite slight quantitative differences, the findings in Fig. 5, B and C, are similar. In 30 μM glycine, there is also stronger inhibitory effect of FBM on the early-peak currents after a prepulse, and the effect of FBM on the late currents remains quite the same whether the 10 μM NMDA prepulse is present or not (Figs. 2C and 5C). Moreover, the inhibitory effect of FBM on the late current directly elicited by 10 μM NMDA during the prepulse is also nearly negligible with 30 μM glycine (data not shown). The NMDA concentration-dependent inhibitory effect of FBM thus is a valid observation for a wide concentration range of glycine. Figure 5D plots the two different sets of inhibitory effect of 10 to 300 μM FBM on late NMDA currents elicited by two different concentrations of NMDA in 0.3 μM glycine. All data points are quantitatively well described by the scheme in Fig. 3B (top) and the K_n, $K_{f,c}$, $K_{f,o}$, and $K_{f,d}$ values obtained in Figs. 4 and 6 (see below and eq. 3). The effect of FBM on NMDA currents thus is dependent on not only the NMDA exposure time but also the NMDA concentration. Both are attributes strongly sustaining a use-dependent inhibitory effect, an important feature for a nonsedative anticonvulsant.

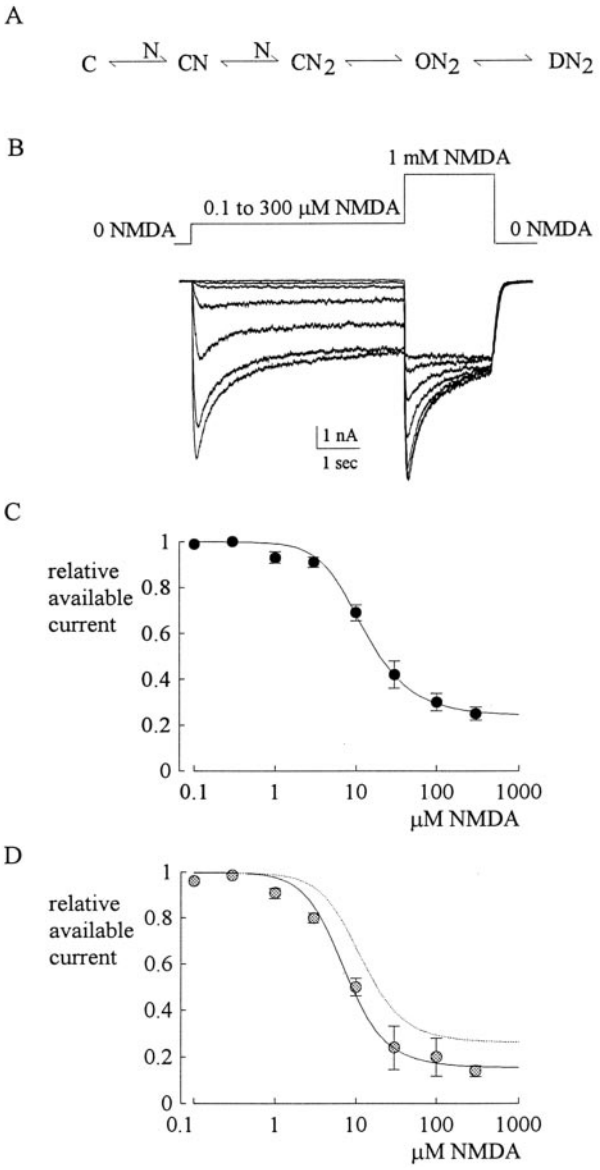

Fig. 6. The desensitization curve of NMDA currents. A, a simplified gating scheme illustrating that binding of two NMDA molecules to the NMDA channels will trigger channel opening as well as desensitization. C, O, and D refer to the closed, open, and desensitized state of the channel, respectively. N refers to the NMDA molecule. CN and CN_2 refer to the closed channels bound with one and two NMDA molecules, respectively. B, every 35 s, the cell was moved from the NMDA- and glycine-free external solution to the external solution containing 0.1 to 300 μM NMDA and 0.3 μM glycine for 5 s (the desensitization prepulse), then moved to another external solution containing 1 mM NMDA and 0.3 μM glycine for 2 s (the test pulse), and then moved back to the NMDA-free external solution again. No FBM is added in this experiment. C, the desensitization curve in control. The peak currents during the test pulse from the experiments in part B are normalized to the peak current elicited by a 2-s 1 mM NMDA pulse without any preceding desensitization pulse in the same cell to give the relative available current. The cumulative results of the relative available current are then plotted against the NMDA concentration in the desensitization prepulse (n = 4–8). The line is the best fit to the mean values using eq. 1 with the m value set at 4 and gives K_n and p values of 34.3 μM and 2.6, respectively. D, the desensitization curves in the external solution containing 300 μM FBM. The experimental protocols are the same as those described in parts B and C, but the external solution here contains 300 μM FBM (n = 4–7). The solid line is the best fit to the mean values using eq. 2, with the same p, K_n, and m values as in part C and r and $K_{f,c}$ values of 8 and 200 μM, respectively. The $K_{f,o}$ value given by the best fit is 110 μM. The broken line is the desensitization curve in control (taken from part C) and is replotted here for comparison.

NMDA Binds to the Resting NMDA Channel with a Dissociation Constant of ~30 μM. We have argued that FBM inhibits NMDA currents by gating modification and "stabilization" of the desensitized NMDA channels. If FBM binds more strongly to the desensitized state than to the resting state, then the steady-state desensitization of the channel in a given concentration of NMDA should be enhanced by FBM. The steady-state desensitization curve plotting the fraction of available channels (i.e., channels not desensitized) against the NMDA concentration therefore should be shifted leftward on the transverse (NMDA concentration) axis. To have a more detailed quantitative analysis of the desensitization curve, we elaborate the simplified model in Fig. 3B (top) into another gating scheme that keeps the basic C-O-D linear motif but incorporates two steps of NMDA binding (Fig. 6A). As a first approximation, we assumed that two NMDA molecules must bind to the NMDA receptor before the channel can open. Also, the two binding sites have the same binding affinity to NMDA, and binding of one NMDA molecule will not affect the binding of the other. The relative steady-state distribution of NMDA receptor channels in states C, CN, CN_2, ON_2, and DN_2 (Fig. 6A) can then be calculated from general rules of simple bimolecular reaction and are 1, $2[N]/K_n$, $([N]/K_n)^2$, $p \times ([N]/K_n)^2$, and $m \times p \times ([N]/K_n)^2$, respectively, where [N] is the NMDA concentration, K_n is the dissociation constant of NMDA binding to either of the two NMDA-binding sites in the closed channel, p is the relative chance that the channel is open (versus staying closed) when both sites are occupied by NMDA, and m is the ratio between the steady-state occupancy of the desensitized state and the open state. The relative available current after steady-state distribution of the channel among different gating states in a fixed concentration of NMDA thus would be:

$$\text{Relative available current} = \frac{(C + CN + CN_2 + ON_2)}{(C + CN + CN_2 + ON_2 + DN_2)}$$

$$= \frac{(1 + (2[N]/K_n) + ([N]/K_n)^2 + p \times ([N]/K_n)^2)}{(1 + (2[N]/K_n) + ([N]/K_n)^2 + (p \times (m + 1) \times ([N]/K_n)^2)} \quad (1)$$

Figure 6C shows the steady-state desensitization data in the control (FBM-free) condition. The relative available current seems to reach a minimum "platform" value of ~0.25 when prepulsed with very high concentrations of NMDA. This finding, along with the finding that the peak current is on average approximately three times the size of the sustained current (e.g., Fig. 2A), suggests an m value no smaller than 2 to 3. This value is very likely to be an underestimate, because some activated channels would be desensitized when the resting channels are still being activated (and the peak current therefore may not exactly represent the total number of channels traversing state ON_2), and also because the current at the end of the 2-s pulse still slightly decays. We therefore set m at 4 while fitting the data points in Fig. 6C with eq. 1 and obtained K_n and p values of 34.3 μM and 2.6, respectively. It is interesting that the K_n value is quite consistent with the previously reported EC_{50} (e.g., ~31–57 μM) (Verdoorn and Dingledine, 1988; Patneau and Mayer, 1990; Sather et al., 1992) or binding affinity (e.g., ~18 μM) (Sather et al., 1992) of NMDA to the NMDA channels despite the different experimental approaches in different studies.

FBM Binds to the Desensitized NMDA Channel with a Dissociation Constant of ~55 μM. We further examined the steady-state NMDA channel desensitization in the presence of 300 μM FBM, which evidently shifts the desensitization curve leftward (Fig. 6D). To minimize the number of free parameters and simplify the fitting procedures, we assume that the resting channels in state C, CN, and CN_2 (Fig. 6A) all have the same affinity to FBM and thus reduce the scheme in Fig. 6A essentially back to that in Fig. 3B (top). With fixed concentrations of NMDA and FBM and general rules of bimolecular reaction, the relative steady-state distribution of NMDA receptor channels in states C, O, D, CF, OF, and DF would be $(1+[N]/K_n)^2$, $p \times ([N]/K_n)^2$, $m \times p \times ([N]/K_n)^2$, $([F]/K_{f,c})(1+[N]/K_n)^2$, $p \times ([F]/K_{f,o})([N]/K_n)^2$, and $m \times p \times ([F]/K_{f,d})([N]/K_n)^2$, respectively, where [F] is FBM concentration, and $K_{f,c}$, $K_{f,o}$, $K_{f,d}$, p, and m have the same meanings as those in Figs. 3B and 6C. The relative available current seems to reach a platform value of ~0.14 when prepulsed with very high concentrations of NMDA in the presence of 300 μM FBM (Fig. 6D). This finding, along with the finding (e.g., Fig. 2A) that the peak current is approximately six times the size of the sustained current in the presence of 1 mM FBM, would suggest that the ratio between the steady-state occupancy of states DF and OF [i.e., $m \times (K_{f,o}/K_{f,d})$, designated as "r"] is no smaller than 5 to 6. This is again very likely to be an underestimate for the same reasons given previously for m >2 to 3 (and also because 300 μM to 1 mM FBM may not be enough to make all NMDA channels FBM-bound). We therefore set r at 8 (which would necessarily set $K_{f,o} = K_{f,d} \times r/m = 2 \times K_{f,d}$ because of microscopic reversibility), and then we have:

$$\text{Relative available current} = (C + O + CF + OF)/(C + O + D + CF + OF + DF) = ((1 + (300/K_{f,c}))(1 + ([N]/K_n))^2 + p(1 + (300/K_{f,o}))([N]/K_n)^2)/((1 + (300/K_{f,c}))(1 + ([N]/K_n))^2 + p(5 + 9(300/K_{f,o}))([N]/K_n)^2) \quad (2)$$

Given $K_{f,c} = 200$ μM from Fig. 4C as well as p = 2.6 and $K_n = 34$ μM from Fig. 6C, the only free parameter in eq. 2 is $K_{f,o}$. The best fit using eq. 2 to the data in Fig. 6D then gives $K_{f,o} = 110$ μM, which would then give a $K_{f,d}$ value of 55 μM. Interestingly, the very different inhibitory effects of FBM on the currents elicited by different concentrations of NMDA in the other experiments such as Fig. 5D can also be well described with the foregoing rationales and the same m, r, K_n, p, $K_{f,c}$, $K_{f,o}$, and $K_{f,d}$ values, namely

$$\text{Relative late sustained current (in the presence of FBM versus in control)} = ((O + OF)/(C + O + D + CF + OF + DF))/(O/(C + O + D)) = (((1 + ([F]/110))(2.6(([N]/34)^2)/(((1 + (([N]/34)^2)(1 + ([F]/200)) + (1 + ([F]/110))(2.6(([N]/34)^2)) + (1 + ([F]/55))(4 \times 2.6(([N]/34)^2))))/((2.6(([N]/34)^2))/(((1 + ([N]/34))^2) + (2.6(([N]/34)^2)) + (4 \times 2.6(([N]/34)^2)))) \quad (3)$$

where [N] is NMDA concentration (i.e., either 10 or 1000 μM in Fig. 5D), and [F] is FBM concentration (the transverse axis in Fig. 5D). The $K_{f,c}$, $K_{f,o}$, and $K_{f,d}$ values (200, 110, and 55 μM, respectively) thus seem to be reasonable estimates that are well consistent with all essential findings from different experiments in this study.

FBM Enhances NMDA Currents in Very Low Concentrations of NMDA. From the foregoing rationales, one may explain the nature of the nearly negligible inhibition of FBM on the currents elicited by 10 μM NMDA (Fig. 5, A and D) in more detail. During the 10 μM NMDA prepulse, ~30% NMDA channels are driven into the desensitized state (Fig. 6C), and this proportion would be increased to ~50% in the presence of 300 μM FBM (Fig. 6D). The peak currents during the subsequent 1 mM NMDA pulse, which is designed to activate most of the available NMDA channels at the end of the 10 μM NMDA prepulse, would therefore be decreased in the presence of FBM because more NMDA channels are stabilized in the desensitized state. On the other hand, with a K_n value of 34 μM, a large number of the available channels should remain in the resting state during the 10 μM NMDA prepulse. The nearly negligible inhibitory effect of FBM during the prepulse therefore must indicate an "adequate" increase of open channels (to compensate for the increased desensitized channels by FBM) in the presence of a large amount of resting channels. In other words, FBM should also bind more tightly to the activated than to the resting state, a conclusion well consistent with the $K_{f,c}$ and $K_{f,o}$ values obtained from Fig. 6. The higher affinity of FBM to the activated channels than to the resting channels could be further evidenced by the effect of 300 μM FBM on the NMDA currents elicited by very low concentrations of NMDA, when most NMDA channels stay in the resting state (Fig. 7). Under such circumstances, FBM actually enhances the NMDA currents, especially the early-peak currents (Fig. 7A). Along with the nearly negligible effect of FBM on the NMDA currents elicited by 10 μM NMDA (Fig. 5B) and the significant inhibitory effect of FBM on the NMDA currents elicited by 1 mM NMDA (Fig. 2), the apparent EC_{50} value of the NMDA concentration-response (defined by the NMDA concentration eliciting half-maximal peak currents in each experimental condition) is changed from ~45 μM (in the absence of FBM) to ~30 μM (in 300 μM FBM, detailed data not shown), as if FBM is an agonist rather than an antagonist of the NMDA channel. For a more quantitative analysis of the enhancement of the NMDA currents elicited by micromolar NMDA, a rough estimate of the opening probability was obtained by the ratio between the peak currents in micromolar NMDA and in 1 mM NMDA (Fig. 7B). The opening probability is then fitted with an equation with rationales similar to those of eq. 1:

$$\text{Opening probability} = (ON_2)/(C + CN + CN_2 + ON_2 + DN_2) = (p \times ([N]/K_n)^2)/(1 + (2[N]/K_n) + ([N]/K_n)^2 + (p \times (m + 1) \times ([N]/K_n)^2)) \quad (4)$$

Given p = 2.6 and m = 4 (values from Fig. 6C), the best fit with eq. 4 to the data points in the control condition gives $K_n = 28$ μM (Fig. 7B), a value fairly close to the K_n obtained from a completely different approach in Fig. 6 (34 μM). With the same fixed parameters, the data in 300 μM FBM can be best fitted with $K_n = 18$ μM, indicating a 1.6-fold change in the affinity of NMDA to the NMDA channel in the presence of

300 μM FBM. Alternatively, one may also fix K_n at 28 μM and fit for p. The best fit to the data in 300 μM FBM then gives p = 5.3, indicating that NMDA-bound channels have roughly twice the chance of opening in 300 μM FBM. These results not only strongly sustain that FBM indeed stabilizes the activated more than the resting NMDA channel but also are quantitatively consistent with the foregoing fitting results in Fig. 6, especially that $K_{f,c}$ is nearly twice as large as $K_{f,o}$.

FBM Delays Recovery from Desensitization in NMDA Channels. We have confirmed the higher affinity of FBM to the open than to the resting NMDA channels. If FBM also selectively binds to and stabilizes the desensitized channel, then the recovery from desensitization most probably would be slowed by FBM. Figure 8 examines the recovery courses in control and in 300 μM FBM. The recovery courses can be reasonably fitted with only two-exponential but not single-exponential functions. The slowing of recovery from desensitization in the presence of 300 μM FBM is not dramatic, but it is definite (i.e., the larger slow component as well as the larger fast τ and slow τ values). Although one should not expect to deduce the exact kinetic changes purely from steady-state data, the modest but definite effect of FBM on the recovery kinetics from desensitization again is consistent with the modest but definite selective binding of FBM to the desensitized than to the resting NMDA channels ($K_{f,d}/K_{f,c}$ = 55/200 μM). By the same token, the findings that FBM causes little changes in the macroscopic deactivation kinetics after an NMDA pulse (e.g., Fig. 2) may also be consistent with an even smaller difference between $K_{f,o}$ and $K_{f,c}$ (110 versus 200 μM) if the recovery of desensitized NMDA channels does not traverse an open state of the channel (compare Kuo and Bean, 1994a).

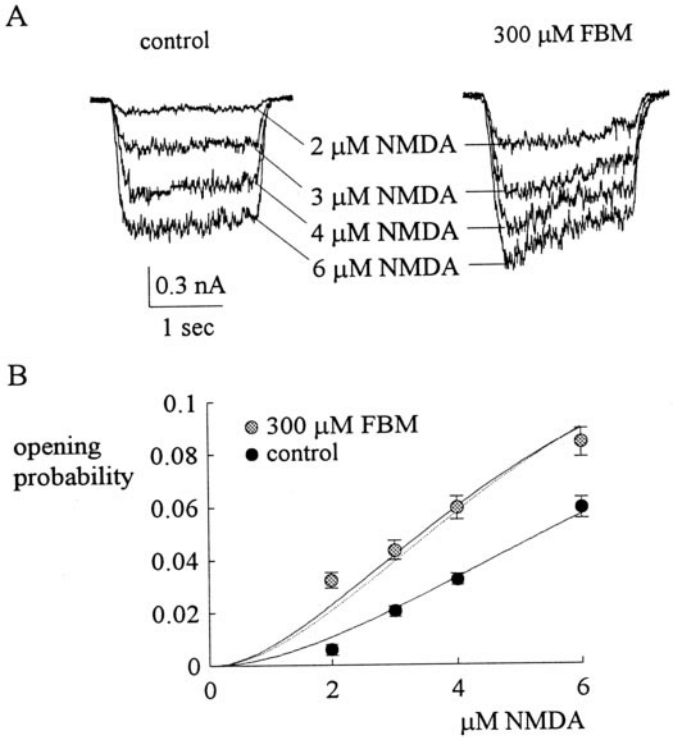

Fig. 7. FBM enhancement of the NMDA currents elicited by low concentrations of NMDA. A, NMDA currents were elicited by the same experimental protocol as that described in Fig. 2, except that micromolar (2–6 μM) NMDA concentrations are also tested in addition to 1 mM. It is evident that the currents are larger in the presence of 300 μM FBM than in control, especially the early-peak currents. B, the opening probability is defined as the ratio between the peak current amplitude in micromolar NMDA pulse and that in 1 mM NMDA pulse and is plotted against the NMDA concentration. The solid lines are best fits to the data points using eq. 4, with p and m values fixed at 2.6 and 4 (the same values as those in Fig. 6), respectively. For the data in the control condition, the K_n value given by the best fit is 28 μM. The best fit to the data in 300 μM FBM gives K_n = 18 μM with the same fixed parameters. We have also fixed K_n at 28 μM and fit the p value for the data in 300 μM FBM. In this latter case, the best fit gives p = 5.3 and a fitting curve (the broken line) very similar to that with p = 2.6 and K_n = 18 μM.

Discussion

Submillimolar FBM Is an Effective Gating Modifier rather than a Pore Blocker of the NMDA Channel. In this study, we showed that submillimolar (0.1–1 mM) FBM effectively alters NMDA currents in mammalian central neu-

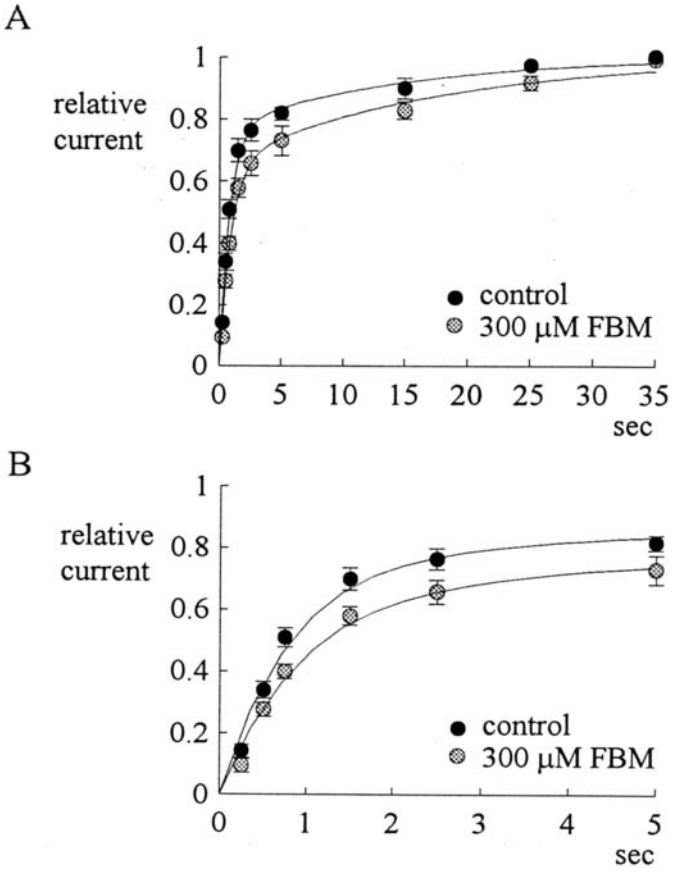

Fig. 8. Delayed recovery of desensitized NMDA channels by FBM. A, every 45 s, the cell was moved from the NMDA- and glycine-free external solution to the external solution containing 1 mM NMDA and 0.3 μM glycine for 2 s, then moved back to the NMDA-free external solution for different period of time (0.5–35 s, the "recovery time"), and then moved again to the 1 mM NMDA external solution to elicit NMDA current from the available channel (i.e., the channel which is not in the desensitized state). The difference between the peak current in the second NMDA pulse and the late current in the first NMDA pulse is normalized to the difference between the peak current and the late current in the first NMDA pulse to give the fraction recovered (FR), which is plotted against the recovery time (T). The lines are two-exponential fits to the data of the following form: FR = 1 − a × exp(−T/τ1) − (1 − a) × exp(−T/τ2). The A, τ1, and τ2 values are 0.77, 0.82 s, and 14.4 s (in the control condition) and 0.66, 0.93 s, and 17.4 s (in 300 μM FBM), respectively. B, the first 5 s of the recovery courses with the fitting curves are redrawn here for a more clear presentation of the early phase of recovery.

rons. FBM has a much stronger inhibitory effect on the late-sustained than on the early-peak NMDA currents (Fig. 2). FBM also accelerates both the activation and the decay phase of NMDA currents. In both cases, the acceleration is more apparent with increasing FBM concentration of up to ~300 μM and then becomes saturated in 300 to 1000 μM FBM (Figs. 3 and 4). Moreover, FBM "paradoxically" enhances the NMDA currents elicited by micromolar NMDA (Fig. 7). These data strongly suggest that submillimolar FBM is chiefly a gating modifier rather than a pore blocker of the NMDA channel, and it modifies channel gating by enhancement of the activation and especially the desensitization processes. In view of the findings that approximately 1 to 3 mM FBM slightly decreased single channel currents and inhibited steady-state binding of [^{3}H]dizocilpine (an open NMDA channel blocker) (Rho et al., 1994; Subramaniam et al., 1995), FBM probably could also block the NMDA channel pore but would require millimolar concentrations to do so.

FBM Significantly Modifies the Resting NMDA Channel in Therapeutic Conditions. We have quantitatively characterized the gating modification of the NMDA channel by FBM and documented different affinity between FBM and different gating states of the channel (200, 110, and 55 μM for $K_{f,c}$, $K_{f,o}$, and $K_{f,d}$, respectively; Fig. 6). In view of the 50 to 300 μM (mean, ~150 μM) therapeutic concentrations of FBM in plasma or brain (Leppik et al., 1991; Theodore et al., 1991; The Felbamate Study Group in Lennox-Gastaut Syndrome, 1993; Adusumalli et al., 1994), a $K_{f,c}$ of 200 μM would imply that a significant proportion (on average, nearly half) of the NMDA channel is already bound and modified by FBM when the neuron is at rest. This is in sharp contrast to the cases of other major anticonvulsants phenytoin, carbamazepine, and lamotrigine, which are Na^+-channel inhibitors and share a common anticonvulsant binding site in the channel (Kuo, 1998). The therapeutic concentrations of these Na^+ channel inhibitors are close to their dissociation constants to the inactivated Na^+ channel but are far smaller than their dissociation constants to the resting channel. Moreover, their binding kinetics to the inactivated Na^+ channel are very slow (Kuo and Bean, 1994b; Kuo et al., 1997; Kuo and Lu, 1997). Thus, phenytoin, carbamazepine, and lamotrigine would significantly bind to and inhibit Na^+ channels only in the presence of excessive neuronal activities or prolonged depolarization. This is an important attribute ensuring negligible effect of these Na^+-channel inhibitors on normal neuronal firings, but it may also weaken their antiepileptic effect against seizure discharges characterized by repetitive short depolarization such as petit mal. Although FBM analogously has a higher affinity to the desensitized NMDA channel, the binding kinetics of FBM to the desensitized NMDA channels during ictal depolarization are less critical because FBM already significantly binds to the resting NMDA channels. The macroscopic NMDA current decays with a time constant of 200 to 300 ms (in control and in 0.1–1 mM FBM) (Figs. 2 and 3). Thus, in the first 50 to 100 ms of an NMDA pulse there might be only small inhibition of the current by FBM (little inhibition of the early peak currents; Fig. 2), but the inhibitory effect would become more apparent within the next 100 to 200 ms. This feature could make FBM more effective against some short ictal discharges than the Na^+-channel inhibitors and thus a more broad-spectrum antiepileptic drug. Kleckner et al. (1999) reported that FBM inhibition of NMDA currents was unlikely to be activity-dependent, because FBM dissociated from NR1-ϵ2 receptors more rapidly than did NMDA. However, this conclusion was taken from experiments in which FBM was given and washed off with NMDA. In the continuous presence of FBM (such as in our experiments and in therapeutic conditions), use-dependent inhibition of the NMDA current is probably always ready to occur because significant FBM binding happens even to the resting NMDA channels, and the FBM-bound channels would have different gating operations during the subsequent NMDA pulses.

The FBM Binding Site in NMDA Channels Undergoes Less Apparent Gating Conformational Changes than the Anticonvulsant Binding Site in Na^+ Channels. Given a $K_{f,c}$ of 200 μM and a $K_{f,d}$ of 55 μM in our experimental conditions, the difference in binding energy between FBM binding to the resting and to the desensitized NMDA channels is only ~1.3 RT (product of gas constant and absolute temperature). In contrast, the binding affinity of phenytoin, carbamazepine, or lamotrigine to the inactivated Na^+ channels is at least ~40- to ~200-fold higher than that to the resting Na^+ channels (Kuo and Bean, 1994b; Kuo et al., 1997; Kuo and Lu, 1997), indicative of a binding energy difference of at least 3.7 - 5.3 RT. The FBM-binding site in NMDA channels thus seems to have less apparent conformational changes during the gating process than the common anticonvulsant binding site in Na^+ channels. This difference is reasonable or even "necessary" because a significant proportion of resting NMDA channels are already bound by FBM in therapeutic conditions. Under such circumstances, if the gating conformational changes in the FBM-binding site in NMDA channels are as dramatic as those in the common anticonvulsant binding site in the Na^+ channel, then there might be significant inhibition of NMDA currents even in the absence of excessive exposure to NMDA. The ~1.3 RT binding energy difference between the two gating states thus is a delicate attribute, small enough to ensure the lack of significant inhibitory effect on normal neurotransmission but large enough to sustain the use-dependent inhibitory effect of FBM on NMDA currents.

FBM Binding Allosterically and Delicately Interacts with the Glycine Site. FBM was found to increase [^{3}H]glycine binding (McCabe et al., 1998) but inhibit [^{3}H]5,7-DCKA (a high-affinity competitive glycine receptor antagonist) (McCabe et al., 1993) binding in the rat brain, although the effects are not dramatic (300 μM FBM produced a ~20% change in both cases). On the other hand, Subramaniam et al. (1995) reported no change in [^{3}H]5,7-DCKA binding by 0.1 to 1 mM FBM. Glycine is an important gating modifier of the NMDA channel. It seems to favor the activated conformation (Johnson and Ascher, 1987; Kleckner and Dingledine, 1988) but decreases desensitization of the NMDA channel (Lerma et al., 1990). According to the different effects of FBM on glycine and 5,7-DCKA binding, it is unlikely that FBM directly binds to the strychnine-insensitive glycine-binding site in the NMDA channel. Instead, FBM binding probably has an allosteric synergistic effect on the glycine site to increase glycine binding, because FBM also favors the activated over the resting conformation of the channel (Figs. 4 and 7). This synergistic effect may not be very strong and is sensitive to small changes in experimental conditions, including ionic concentrations (McCabe et al., 1998). On the other hand,

NMDA channel desensitization may decrease glycine (in view of the decreased desensitization by glycine) (Lerma et al., 1990) but increase FBM binding (in view of the smaller $K_{f,d}$ than $K_{f,o}$). FBM thus may also have an allosteric antagonistic effect on glycine binding. The two possible opposing interactions between glycine and FBM may also explain why the effects of FBM are roughly similar in 30 and 0.3 μM glycine (Figs. 2, B and C, and 5, B and C). Although 5,7-DCKA binds to the glycine site, the conformational requirements for its binding may not be exactly the same as those of glycine, and the effect of channel desensitization on 5,7-DCKA and glycine binding could be different. Along with the possibilities of different distribution in gating states in different studies, the seemingly complicated or even conflicting previous reports might be explained.

FBM and Phenylethanolamines Have Similar Actions but Probably Different Binding Ligands on the NMDA Channel Protein. Ifenprodil and other phenylethanolamines also show activity-dependent inhibition of the NMDA currents (Gallagher et al., 1996; Kew et al., 1996; Mott et al., 1998). Like FBM, ifenprodil has a dose-dependent inhibitory effect in 3 to 30 μM NMDA but enhances NMDA currents when the NMDA concentration is extremely low (0.3 to 1 μM) (Kew et al., 1996). Both FBM and ifenprodil thus probably favor the major conformational changes induced by NMDA on NMDA channels, namely activation and desensitization. The high-affinity ifenprodil-binding site has been located to the amino terminal region of NR2B subunit (especially involving Arg337) (Gallagher et al., 1996), a region probably also controlling NMDA channel desensitization (the LIVBP-like domain) (Krupp et al., 1998). Interestingly, FBM also has a stronger effect on channels containing NR2B than those containing NR2A or NR2C subunit (Kleckner et al., 1999). However, Kleckner et al. (1999) found that some mutations in the amino terminal of NR2B subunit significantly affect ifenprodil but not FBM binding, suggesting that FBM and ifenprodil do not bind to exactly the same amino acids in the NMDA channel protein. It is possible that similar gating conformational changes of the glutamate receptor (e.g., channel activation) could be favored by binding of different ligands either to different areas (e.g., glutamate and glycine) or to different amino acids in the same area (e.g., glutamate and kainite) (Pass et al., 1996; Sutcliffe et al., 1996; Swanson et al., 1997; Armstrong et al., 1998). Further exploration of the binding sites of FBM and ifenprodil would not only be of pharmacological interest but also shed light on the gating conformational changes of the NMDA channel protein.

References

Adusumalli VE, Wichmann JK, Kucharczyk N, Kamin M, Sofia RD, French J, Sperling M, Bourgeois B, Devinsky O, Dreifuss FE, et al. (1994) Drug concentration in human brain tissues from epileptic patients treated with felbamate. *Drug Metab Dispos* **22:**168–170.

Armstrong N, Sun Y, Chen G-Q, and Gouaux E (1998) Structure of a glutamate-receptor ligand-binding core in complex with kainate. *Nature (Lond)* **395:**913–917.

Colquhoun D and Hawkes AG (1995) Desensitization of *N*-methyl-D aspartate receptors: a problem of interpretation. *Proc Natl Acad Sci USA* **92:**10327–10329.

The Felbamate Study Group in Lennox-Gastaut Syndrome (1993) Efficacy of felbamate in childhood epileptic encephalopathy (Lennox-Gastaut syndrome). *N Engl J Med* **328:**29–33.

Gallagher MJ, Huang H, Pritchett DR, and Lynch DR (1996) Interactions between ifenprodil and the NR2B subunit of the *N*-methyl-D-aspartate receptor. *J Biol Chem* **271:**9603–9611.

Johnson JW and Ascher P (1987) Glycine potentiates the NMDA response in cultured mouse brain neurons. *Nature (Lond)* **325:**529–531.

Kanthasamy AG, Matsumoto RR, Gunasekar PG, and Truong DD (1995) Excitoprotective effect of felbamate in cultured neurons. *Brain Res* **705:**97–104.

Kaufman DW, Kelly JP, Anderson T, Harmon DC, and Shapiro S (1997) Evaluation of case reports of aplastic anemia among patients treated with felbamate. *Epilepsia* **38:**1265–1269.

Kew JNC, Trube G, and Kemp JA (1996) A novel mechanism of activity-dependent NMDA receptor antagonism describes the effect of ifenprodil in rat cultured cortical neurons. *J Physiol* **497:**761–772.

Kleckner NW and Dingledine RD (1988) Requirement for glycine in activation of NMDA receptors expressed in *Xenopus* oocytes. *Science (Wash DC)* **241:**835–837.

Kleckner NW, Glazewski JC, Chen CC, and Moscrip TD (1999) Subtype-selective antagonism of *N*-methyl-D-aspartate receptors by felbamate: insights into the mechanism of action. *J Pharmacol Exp Ther* **289:**886–894.

Krupp JJ, Vissel B, Heinemann SF, and Westbrook GL (1998) N-terminal domains in the NR2 subunit control desensitization of NMDA receptors. *Neuron* **20:**317–327.

Kuo C-C (1998) A common anticonvulsant binding site for phenytoin, carbamazepine and lamotrigine in neuronal Na^+ channels. *Mol Pharmacol* **54:**712–721.

Kuo C-C and Bean BP (1994a) Na^+ channels must deactivate to recover from inactivation. *Neuron* **12:**819–829.

Kuo C-C and Bean BP (1994b) Slow binding of phenytoin to inactivated sodium channels in rat hippocampal neurons. *Mol Pharmacol* **46:**716–725.

Kuo C-C, Chen R-S, Lu L, and Chen R-C (1997) Carbamazepine inhibition of neuronal Na^+ currents: quantitative distinction from phenytoin and possible therapeutic implications. *Mol Pharmacol* **51:**1077–1083.

Kuo C-C and Lu L (1997) Characterization of lamotrigine inhibition of Na^+ channels in rat hippocampal neurons. *Br J Pharmacol* **121:**1231–1238.

Leppik IE, Dreifuss FE, Pledger GW, Graves NM, Santilli N, Drury I, Tsay JY, Jacobs MP, Bertram E, Cereghino JJ, et al. (1991) Felbamate for partial seizures: results of a controlled clinical trial. *Neurology* **41:**1785–1789.

Lerma J, Zukin RS, and Bennett MVL (1990) Glycine decreases desensitization of *N*-methyl-D-aspartate (NMDA) receptors expressed in *Xenopus* oocytes and is required for NMDA responses. *Proc Natl Acad Sci* **87:**2354–2358.

Lin F and Stevens CF (1994) Both open and closed NMDA receptor channels desensitize. *J Neurosci* **14:**2153–2160.

McCabe RT, Sofia RD, Layer RT, Leiner KA, Faull RLM, Narang N, and Wamsley JK (1998) Felbamate increases [^{3}H]glycine binding in rat brain and sections of human postmortem brain. *J Pharmacol Exp Ther* **286:**991–999.

McCabe RT, Wasterlain CG, Kucharczyk N, Sofia RD, and Vogel JR (1993) Evidence for anticonvulsant and neuroprotectant action of felbamate mediated by strychnine-insensitive glycine receptors. *J Pharmacol Exp Ther* **264:**1248–1252.

Mott DD, Doherty JJ, Zhang S, Washburn MS, Fendley MJ, Lyuboslavsky P, Traynelis SF, and Dingledine R (1998) Phenylethanolamines inhibit NMDA receptors by enhancing proton inhibition. *Nat Neurosci* **1:**659–667.

Pass Y, Eisenstein M, Medevielle F, Teichberg VI, and Devillers-Thiery A (1996) Identification of the amino acid subsets accounting for the ligand binding specificity of a glutamate receptor. *Neuron* **17:**979–990.

Patneau DK and Mayer ML (1990) Structure-activity relationships for amino acid transmitter candidates acting at *N*-methyl-D-aspartate and quisqualate receptors. *J Neurosci* **10:**2385–2399.

Pellock JM (1999) Felbamate. *Epilepsia* **40:**S57–S62.

Pellock JM and Brodie MJ (1997) Felbamate: 1997 update. *Epilepsia* **38:**1261–1264.

Pugliese AM, Passani MB, Pepeu G, and Corradetti R (1996) Felbamate decreases synaptic transmission in the CA1 region of rat hippocampal slices. *J Pharmacol Exp Ther* **279:**1100–1108.

Rho JM, Donevan SD, and Rogawski MA (1994) Mechanism of action of the anticonvulsant felbamate: opposing effects on *N*-methyl-D-aspartate and GABA-A receptors. *Ann Neurol* **35:**229–234.

Rho JM, Donevan SD, and Rogawski MA (1997) Barbiturate-like actions of the propanediol dicarbamates felbamate and meprobamate. *J Pharmacol Exp Ther* **280:**1383–1391.

Sather W, Dieudonne S, MacDonald JF, and Ascher P (1992) Activation and desensitization of *N*-methyl-D-aspartate receptors in nucleated outside-out patches from mouse neurons. *J Physiol* **450:**643–672.

Stefani A, Calabresi P, Pisani A, Mercuri NB, Siniscalchi A, and Bernardi G (1996) Felbamate inhibits dihydropyridine-sensitive calcium channels in central neurons. *J Pharmacol Exp Ther* **277:**121–127.

Subramaniam S, Rho JM, Penix L, Donevan SD, Fielding RP, and Rogawski MA (1995) Felbamate block of the *N*-methyl-D-aspartate receptor. *J Pharmacol Exp Ther* **273:**878–886.

Sutcliffe MJ, Wo ZG, and Oswald RE (1996) Three-dimensional models of non-NMDA glutamate receptors. *Biophys J* **70:**1575–1589.

Swanson GT, Gereau IVRW, Green T, and Heinemann SF (1997) Identification of amino acid residues that control functional behavior in GluR5 and GluR6 kainate receptors. *Neuron* **19:**913–926.

Swinyard EA, Sofia RD, and Kupferberg HJ (1986) Comparative anticonvulsant activity and neurotoxicity of felbamate and four prototype-antiepileptic drugs in mice and rats. *Epilepsia* **27:**27–34.

Taglialatela M, Ongini E, Brown AM, Di Renzo G, and Annunziato L (1996) Felbamate inhibits cloned voltage-dependent Na^+ channels from human and rat brain. *Eur J Pharmacol* **316:**373–377.

Theodore WH, Raubertas RF, Porter RJ, Nice F, Devinsky O, Reeves P, Bromfield E, Ito B, and Balish M (1991) Felbamate: a clinical trial for complex partial seizures. *Epilepsia* **32:**392–397.

Verdoorn TA and Dingledine R (1988) Excitatory amino acid receptors expressed in *Xenopus* oocytes: agonist pharmacology. *Mol Pharmacol* **34:**298–307.

Address correspondence to: Dr. Chung-Chin Kuo, Department of Physiology, National Taiwan University College of Medicine, 1, Jen-Ai Road, 1st Section, Taipei, 100, Taiwan. E-mail: cckuo@ha.mc.ntu.edu.tw